EUROPEAN ORGANIZATION FOR NUCLEAR RESEARCH
European Laboratory for Particle Physics

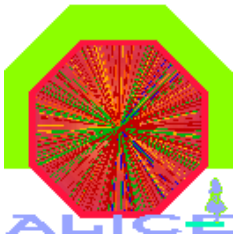

IPN Paris,
INFN Cagliari,
VECC Calcutta

Internal Note/Muon Arm

ALICE reference number
ALICE-INT-2005-008 version 1.0
Institute reference number
[-]
Date of last change
February 2005

Radiation studies for the Readout Electronic of the ALICE Dimuon Forward Spectrometer

Authors:

C. Suire¶, A. Charpy, V. Chambert, M.P. Comets, P. Courtat, B. Espagnon, R. Kunne, Y. Le Bornec, J.M. Martin, S. Rousseau, N. Willis.
Institut de Physique Nucléaire (IPN) - IN2P3/CNRS - Université Paris XI

M. Arba, D. Marras, G. Usai.
Istituto Nazionale di Fisica Nucleare (INFN), Sezione di Cagliari

S.K. Pal
Variable Energy Cyclotron Center
Kolkata

Abstract:

The Dimuon Forward Spectrometer (DFS) of the ALICE detector has entered the construction phase; nevertheless the validation of some specific parts of the Front End Electronic (FEE) and Data Acquisition (DAQ) still need to be done. Pre-production runs of the final components of the FEE have been made; the radiation hardness of these latest versions of the electronics have to be tested.
In the first part of this note, a review (from the literature on irradiation) of results, relative to the FEE and DAQ components, is presented. An extrapolation of these results to the ALICE environment is attempted.
In the second part, we describe the irradiation tests performed at Orsay for the main components of the FEE, i.e. the MANAS readout chip and the MARC ASIC. Results are presented and discussed.

¶Corresponding author : suire@in2p3.fr

1 Introduction

A Large Ion Collider Experiment (ALICE) [ALI] is in preparation at LHC. It is a complex apparatus aimed at the detection of hadrons, leptons and photons emitted in the Pb+Pb collisions at ultra-relativistic energies (see also table 3). The ALICE experiment will study the properties of strongly interacting matter at high densities, where a new phase of a matter called Quark-Gluon Plasma (QGP) is expected to live a significant amount of time and thus being studied. Recent results from the Relativistic Heavy Ion Collider experiments [RHIC] at Quark Matter conference [QM04] have already shown really convincing hints, if not evidences, of the creation of such a state. A particularly interesting probe to study the QGP is the evolution of the production of vector mesons J/Ψ [NA50], Ψ', ϒ, ϒ' ϒ": observing the muonic decay of these mesons is the task assigned to the dimuon forward spectrometer.

The dimuon forward spectrometer covers the pseudo-rapidity range from $\eta = 2.5$ to 4.0 (see fig.1).

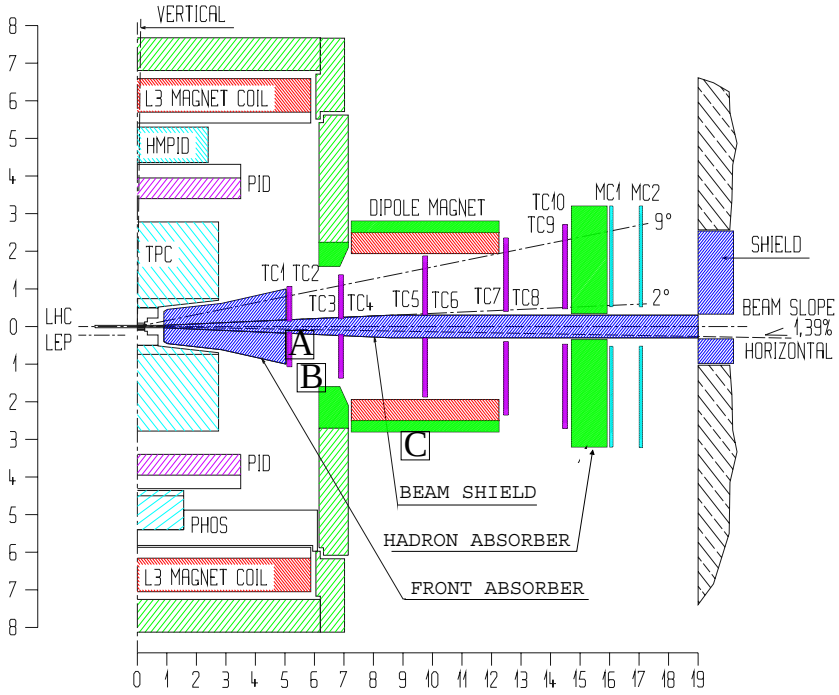

* **acceptance:**	θ = 2° − 9	η = 2.5− 4
* **front absorber**	≈11λ C +Concrete	heavy metal shield (W or Pb)
* **beam shield**	θ < 2°, r_i = 4cm, r_o < 29 cm	heavy metal (mainly Pb)
* **dipole magnet**	B=0.7T, Bl = 3 Tm	r = 1.9 m
* **tracking chambers**	10 logical planes,	high resolution & granularity
* **hadron absorber**	≈11λ Fe	
* **trigger chambers**	4 logical planes,	low resolution & granularity

Figure 1: Scheme -side view- of the dimuon forward spectrometer. The Alice detector is partially visible on the left side of the drawing. Labels A, B and C will be explained in the following section.

In order to isolate the signal from muon pairs, the hadronic background has to be filtered

off; thus an absorber has been placed in front of the detector to stop the pions, protons and kaons emerging from the collisions. One can also notice that the beam pipe all along the detector is surrounded by a shielding devoted to absorb hadrons (π, K) produced at small angle.

The detection/tracking system consists of 10 planes of wire chambers divided into 5 stations; each detection plane provides (X,Y) coordinates of a crossing particle. Planes 5 and 6 are operated in the Dipole Magnet (see Fig.1), which produces a 0.7 T magnetic field used to bend the trajectory of charged particles allowing the determination of their momentum. The mass resolution on J/Ψ or Υ mesons is naturally dependent on the resolution of the chambers which must stay below 100 μm together with a high single plane detection efficiency (99% for charged particles).

	Inner diameter (mm)	Outer diameter (mm)	Position (mm)	Number of channels
Station 1	364	1766	5400	230400
Station 2	464	2238	6860	225280
Station 3	660	3166	9750	157184
Station 4	670	4405	12490	220160
Station 5	670	5132	14490	243200

Table 1: Active areas and number of channels for the five stations of the dimuon forward spectrometer.

The purpose of these tests is to validate, in terms of radiation hardness, the readout electronics of the DFS to insure that it will handle the dose foreseen in the ALICE experiment. Radiation damages may have an impact on the final reconstruction of the tracks (signal discrimination, losses of readout chip generating dead areas, etc...) and thus on the expected physics performances.

2 The Dimuon Forward Spectrometer Electronic

2.1 General Overview

A schematic view of the readout chain can be seen on figure 2. Signal on the cathodes of the pad chambers are read by the MANU (MAnas NUmerical) boards, which are identical for the entire DFS in terms of functionalities and components. The main difference is the size of the MANU board; slightly smaller for stations 1 and 2 than for stations 3, 4 and 5. On each board, 4 MANAS (Multiplexed ANAlogic Signal processor) perform the pre-amplification, filtering and shaping of the signal. The multiplexed output of two consecutive MANAS is digitized by a 12 bits ADC. The handling of the sequences is done by an ASIC, the Muon Arm Readout Chip (MARC) which also performs the zero suppression and the communication with the DSPs (Digital Signal Processor) in charge of the readout. The values of the non null digitized charges are then transmitted by digital local buses toward the PATCH (Protocol for Alice Tracking Chambers) buses.

DSP farms will achieve the readout of the data coming from the FEE. These DSPs are grouped in *clusters* in 20 specific crates called CROCUS (Cluster Read Out Concentrator Unit System). Each crate, located outside the detector acceptance, is composed of :

- 5 boards called *frontal* directly connected to the PATCH buses by ribbon cables,
- one concentrator board which collects the data coming from all the frontal boards. After formatting, data are transmitted to the SIU (Source Interface Unit) which will achieve the transmission toward the DDL (Detector Data Link).

The trigger signals coming from the CTP (Central Trigger Processor) are decoded in a VME card called FFT (Frontal Fan-out Trigger) and then distributed in the FFD (Frontal Fan-out Dispatching) boards. Finally the trigger signal is sent to the 1 100 000 channels with the proper delay depending on their location.

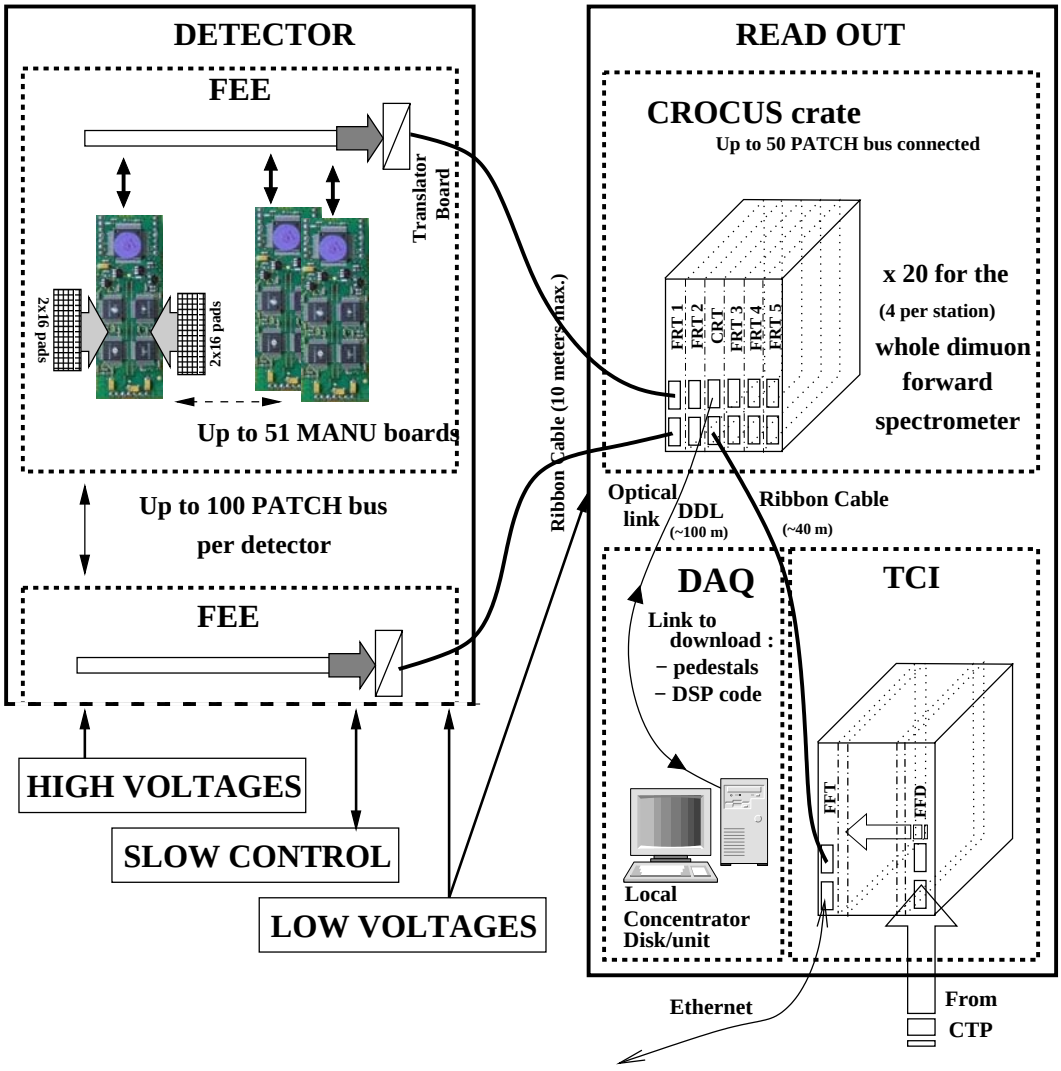

Figure 2: Schematic of the readout chain for the dimuon forward spectrometer.

2.2 Front End Electronic : the MANU board

The MANU boards is the FEE part that will be the most exposed to radiation; even though the particle fluences, thanks to the absorber, are much lower than the ones in the central region of the ALICE detector.

One of the critical components is the MANAS readout chip; degradation of its performances may have dramatic effects on the track reconstruction and thus limiting the detector ability to fulfill the required physics performances. From a technical point of view, the MANAS, manufactured by SCL[1], is a custom IC using 1.2 μm CMOS technology. It has 16 input channels, charge sensitive, and delivers a multiplexed output voltage. It also has built-in capacitors of 0.2 pF for calibration purposes. Irradiation test will include the study of the pedestal, the noise and the gain variations versus the TID (Total Integrated Dose, see Annexe A) and the sensitivity to latch-up if any. The MANAS chip is presented in a TQFP[2] 48 pins and will be tested in it. The die size of the IC is 4.75 mm $\times$ 3.06 mm and the thickness is 675 μm, which is afterward reduced to 375 μm.

The other critical component on a MANU board is the MARC (ASIC). This chip, studied by Cagliari (INFN), has been made in the AMS 0.6 μm, 3.3 V technology. Sensitivity to SEU and SEL (Single Event Upsets and Single Event Latchup, described in Annexe A) need to be estimate.

Other components located on a MANU board will require irradiation tests, namely : ADC AD7476, AD Ref192 and the amplifier Fairchild KM4110 (see table 4). Degradation of these components could also have an impact on the boards operation but no strong effects with respect to the dose are expected.

2.3 CROCUS and TCI crates

The boards in the CROCUS and TCI crates use the same devices; mostly DSPs, FPGAs and EPROMs (Tab. 4). Radiation levels are much lower that the ones expected for the MANU boards (see next section). This kind of devices offers usually a good resistance to TID (up to a few tens of kRad); their sensitivity to SEU is, in this case, the relevant characteristic since SEUs may require a re-initialization of the components. Thus, if the SEU cross section is too important, we might face problems of dead time, due to the large number of these components.

Testing of the DSPs will demand a particular attention since these devices, rarely used in a radiation environment, might be very sensitive to SEU.

3 Radiations levels for ALICE Dimuon Forward Spectrometer

3.1 Expected doses and fluxes in the ALICE environment

Simulations have been made to estimate the doses and hadrons fluences in the ALICE detector; recently, a review of the radiation levels expected in ALICE has been updated [Mor02] and

Tracking Chamber	1/2	3/4	5/6	7/8	9/10
Hadrons Fluences [10^{11} cm^{-2}]	5.6	4.1	1.3	0.9	1.0
Dose [Rad]	500	360	100	50	40

Table 2: Hadrons fluences and doses expected in the stations of the dimuon forward spectrometer.

will be used as a reference for our studies (see Tab 2). These fluences/doses take everything into account; beam-beam and beam-gas collisions as well as the beam halo. In table 3 are

[1]Semiconductor Complex Limited located in India.

[2]Thin Quad Flat Pack, see description in Annexe A.

shown typical numbers of the Physics program for the ALICE experiment for the different colliding systems; these numbers are based on 10 years running period. Over this period, the experiment will be running data during 8 months (7 month of pp collisions, 1 month of PbPb collisions and 4 months of winter shutdown). Considering 1.1×10^7 s of effective run time, it correspond to $\sim$ 11 hours of data taking per day.

	p+p	pPb	Ar+Ar	Ca+Ca	Pb+Pb
$< L >$ [cm^{-2}s^{-1}]	3.0×10^{30}	1.0×10^{29}	3.0×10^{27}	1.0×10^{29}	1.0×10^{27}
$\sigma_{\rm in}$ [mb]	70	1900	3000	3000	8000
Rate [s^{-1}]	2.0×10^5	2.0×10^5	9.0×10^3	3.0×10^5	8.0×10^3
Run Time [s]	1.0×10^8	2.0×10^6	1.0×10^6	2.0×10^6	5.0×10^6
Events	2.0×10^{13}	4.0×10^{11}	9.0×10^9	6.0×10^{11}	4.0×10^{10}
$\sqrt{(s_{NN})}$ [TeV/n]	14	8.8	6.3	6.3	5.6
Particles/event	100	300	2400	2400	14200

Table 3: Beam scenario in ALICE for 10 years of running.

On figure 1, labels **A**, **B** and **C** have been added to the drawing to locate the DFS electronic positions.

Location A: Front End Electronics (all the components of a MANU board) and Translator Boards. The maximum TID is estimated at 5 Gy (500 Rad, see Annexe A) and the hadron fluence at 5.6×10^{11} cm^{-2}. In the DFS, the ratio of neutrons to charged particles is assume to be close to 100; so neutrons will be the most important component of the radiation environment. Gammas are also expected at the level of 10% of the neutron fluence. The TID/fluence is of course the highest for the first station; values decrease with respect to the position of the station along the beam axis.

Location B: CROCUS crates. We can (safely) consider the same fluences as in location **A**; a rough estimation lead to doses and fluences that would be a third of the ones expected in location **A** i.e. a dose of $\sim$ 170 Rad and a hadron fluence of 1.9×10^{11} cm^{-2} (latest simulations gave lower values, TID $\sim$ 100 Rad and $\Phi_h \sim 3.0 \times 10^{10}$ cm^{-2} [Mor04]; the highest values will be used in the following).

Location C: CTI crates (close to the Dipole Magnet). A maximum dose of 1.4 Rad and a neutron fluence of 2.6×10^8 cm^{-2} are expected. These low radiation levels are not worrisome and no dedicated tests will be performed (all the components of the CTI crates are also used in the CROCUS crates and thus will be tested at higher dose/fluence).

The energy spectra of the particles is also an important factor; neutrons, the most abundant specie in the detector acceptance, will induce different reactions depending on their energy. On figure 3, the energy spectra of neutrons is shown for the five stations as well as for the trigger chambers. Three regimes have also been separated $E_n \leq 2$ MeV, 2 MeV $< E_n \leq$ 20 MeV and $E_n >$ 20 MeV (shaded areas, going from the left to the right).

They respectively represent a percentage of 90%, 8.4 % and 1.6 % of the total fluence. A very complete and interesting discussion about the effects of neutrons over this broad energy range can be found in [Huh00]. The authors conclude that a test using a 60-200 MeV proton beam to irradiate the devices should provide a reasonable estimate of the SEU rate in most locations around the LHC. The SEU cross section observed in a medium energy proton beam

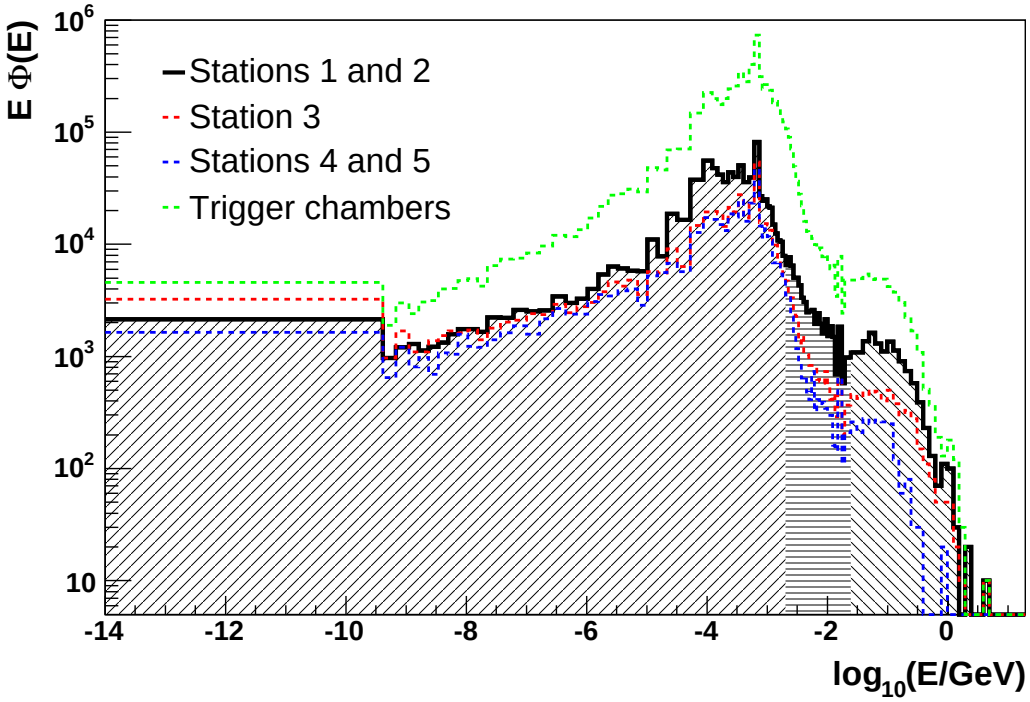

Figure 3: Energy spectra of neutrons in the dimuon forward spectrometer (see text for explanations about shaded areas).

should be applied to the LHC hadron flux above 20 MeV. Or if a conservative estimate is desired this cut could be lowered down to 2 MeV [3].

We can therefore conclude that **only 10% of the total hadron fluence will contribute** and should be taken into account; so in the following section where estimation on the SEUs rate are made, we will use the value of $\Phi^A = 5.6 \times 10^{10}$ cm^{-2} and $\Phi^B = 1.9 \times 10^{10}$ cm^{-2} for the total hadron fluence depending on the location.

3.2 Other experiments studies

Some of the electronic devices (passive and active) used for the readout of the DFS have already been tested by others experiments during their R&D ; for instance, CMS or AMS need complete irradiation studies for each electronic component due to the LHC pp or Space environment. In the table 4, we tried to summarize the available results related to the DFS readout electronic. In the following discussion, all the extrapolated values are relative to the first station only.

ADC AD7476 (from Analog Devices): 4 ADCs of this type were tested [Tim01]. In terms of TID, this device shows a current increase of 6% (after ageing) after receiving a total dose of 30 kRad (220 Rad/min). Functionalities of all four were tested before

[3] *thermal* neutrons ($E_n \leq 2$ MeV) are important only through the reaction ^{10}B(n,α)^{7}Li; the maximum energy of the products is respectively 1.79 and 1.01 MeV and thus a possible energy deposition of a few keV per micron of path length. Even though this energy is certainly sufficient to trigger SEU in some devices, it is not believed to play a major role (for the hypothesis of a low boron concentration).

MANU Boards		
MANAS [14432]	ALICE DFS	this test campaign
MARC [3608]	ALICE DFS	this test campaign
ADC AD7476 [7216]	AMS [Tim01]	TID (Co^{60}) and SE (heavy ions)
AD Ref192 [3608]	ALICE DFS	this test campaign
Amplifier Fairchild KM4110 [7216]	ALICE DFS	to be tested
CROCUS Crates		
DSP AD 21160M(and 21160N) [56]	ALICE DFS	to be tested
Eprom Xilinx XC18V02 [48]	ALICE DFS	to be tested
Eprom AMD AM29LV040 [44]	CMS [Bun03]	SE (30 & 50 MeV protons)
FPGA Xilinx Virtex E [8]	ALICE DFS	to be tested
FPGA Xilinx Spartan IIE [40]	CMS [Bun03]	SE (30 & 50 MeV protons)
EPLD Xilinx XC9536XL [4]	CMS [Lin00]	TID and SE (63 MeV protons)
CTI Crates		
Same components as CROCUS, numbers are respectively [10],[12],[10],[0],[12],[0]		

Table 4: Bibliography on irradiation test results on the dimuon forward spectrometer electronic components (in brackets, the total number necessary to fully equip the first station).

and after irradiation, and no errors were detected. For SEU (SEL), the maximum cross section, for a LET (Linear Energy Transfer) equal to 40 MeVcm^{2}mg^{-1} which is a considerably high value, has been determined to be $\sigma \approx 0.9 \times 10^{-6}$ cm^2 (1.1×10^{-6} cm^2) with a threshold of 5.9 MeVcm^{2}mg^{-1} (15.9 MeVcm^{2}mg^{-1}). These latest results have been obtained by using heavy ions beams, and they cannot be extrapolated to the radiation environment (high energy hadrons) expected in ALICE (see Annexe B).

As an example, a similar component from Analog Device (ADC AD9225) has been tested for the CMS endcap muon detector [Lin00]. This device was irradiated with a proton (63 MeV) fluence of 2.7×10^{12} cm^{-2}, and no SEL was observed.

ALICE radiation environment at location **A** can be described with a TID of 500 Rad and a hadron (E>2 MeV) fluence $\Phi^A = 5.6 \times 10^{10}$ cm^{-2}. According to these numbers, the TID is not critical at all for this component. Conclusion about SEU/SEL are harder to draw; it seems that we can expect a very low rate but this will need to be confirmed in the future.

Eprom AMD AM29LV040: The EPROM used for the DFS is slightly different that the one tested by CMS, the AM29LV160D (the difference being related to the memory size, 16 Mbits for the CMS one) we will nevertheless use these results for our extrapolation. They've shown that all three tested memories survived the irradiation without any errors up to a fluence of 1.2×10^{11} cm^{-2} (beam intensity was 6.7×10^7 cm^{-2}s^{-1}). Errors did occur only when a higher beam intensity (x 50) has been used starting after a fluence of $\sim 6 \times 10^{11}$ cm^{-2}. They also performed tests a few days after the irradiation and observed a correct behavior (in terms of stored and programmed data) of the ICs (for one of the chip, the erase functionality has been destroyed during the irradiation and could not be recovered). Note that the equivalent TID for this proton fluence/energy is a few tens of kRad.

The SEU cross section is certainly lower than $\sigma \sim 0.8 \times 10^{-11}$ cm^2; considering the hadron flux at the location **B**, $\Phi^B = 1.9 \times 10^{10}$ cm^{-2} the SEU rate should not exceed 0.15 per device over a 10 years period (42 months of data taking). Taking into account the 44 Eproms, we obtain approximately 7 SEUs during the whole lifetime of ALICE, having no impact on the dimuon forward spectrometer operating (for the 10 devices located in **C** the SEU rate is completely negligible).

So it is reasonable to believe that this component (areas B and C) will handle without problem the ALICE environment. Testing the exact same component might be useful as a confirmation, but it doesn't seems to be critical at all.

FPGA Xilinx Spartan IIE: the tested device was a Xilinx-IIE (XC2S300E) made in 0.18 μm technology (6912 logic cells, 1875648 configuration bits and 1.8 V power supply). In order to fully test the FPGA functionalities, they performed tests with read-back to check bit errors on the configuration and tests of dedicated logic. In order to separate configuration and dynamic errors, a low beam intensity ($\sim\ 7.5 \times 10^6$ cm^{-2}s^{-1}) was used. The SEU for configuration errors for 30 MeV protons is $\sigma \sim 2.0 \times 10^{-10}$ cm^2 (about 15% higher for 50 MeV protons). Dynamic SEU were tested by configuring the FPGA with a design containing 5504 shift registers (90% of the FPGA resources) and by comparing the input pattern to the output one; no dynamic SEU were observed (independently of the frequency 24 or 100 MHz).

The SEU cross section for this device is 2.3×10^{-10} cm^2. We obtain (with $\Phi^B \sim 1.9 \times 10^9$ cm^{-2}) a total of 175 SEUs over the whole running period considering 40 components of this kind; this represents 1 SEU every 7 days of data taking. We can consider this SEU rate negligible and thus include this FPGA in our readout chain.

EPLD Xilinx XC9536XL: 2 ICs were tested and received approximately the same proton fluence ($\sim\ 3 \times 10^{12}$). It corresponds to a dose of about 40 kRad. No SEL was observed for either chip and the reported SEU cross section is $\sigma = 3.8 \times 10^{-10}$ cm^2. All SEUs were recoverable by reloading the EPLD.

The four components of this kind are located in the **B** area. We still use the very conservative value of 1.9×10^{10} cm^{-2} for the fluence, and the total number of SEUs is 30 over 10 years of running (or less than 1 SEU per month of data taking). This is negligible and thus validate the EPLD Xilinx XC9536XL for our application.

3.3 Summary

In this first part, a general presentation of the ALICE dimuon forward spectrometer and its readout electronics has been given. We also used the latest simulation results to give a description of the expected radiation levels. Irradiation tests results available in the literature allowed us to make extrapolation for components of our readout chain, mainly related to the DAQ. To be complete, irradiation tests of the CROCUS boards will be necessary. These tests will probably take place during 2005 ; from july to november 2004, beam test of the full readout chain including DAQ was the first priority.

The components of the FEE have been specially developed and designed for the dimuon forward spectrometer (MANAS and MARC) thus dedicated irradiation tests are required to characterize their behaviors under radiation. These tests are presented in the following part.

4 Experimental Test Setup

4.1 Description

The experimental setup is represented on Fig.4. The proton beam is delivered by the CPO (Centre de Protonthérapie d'Orsay) [CPO] which also provides an accurate measurement of the fluence (see next section). The control and monitoring of the DUT (Device Under Test) is made via a PC, located about 20 meters away from the experimental area, from which a dedicated software allows us to take full control (display and commands) of the DAQ + Control PC located in the experimental area; all tests programs being actually run from this later one. In oder to control and monitor the voltmeter and the power supply, LabView programs using RS-232 protocol have been used. An analysis program has also been developed to have an

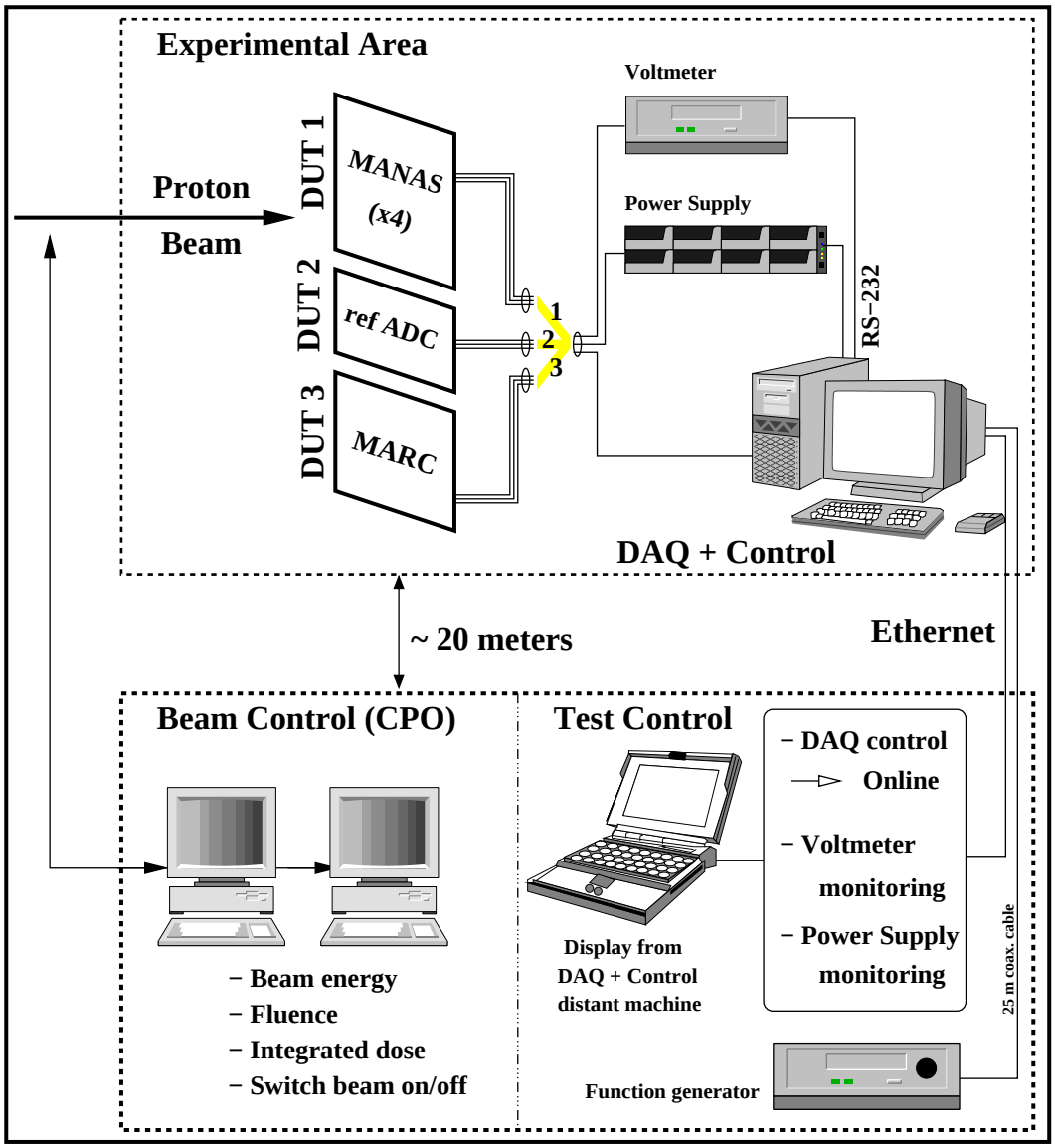

Figure 4: Experimental setup for irradiation tests at CPO.

immediate feedback in terms of data quality and behavior of the tested components.

Depending on the DUT, different measurements have been planned:

- DUT 1 : MANAS on a MANU board. Data are taken after each irradiation (beam was switched on for periods going from 10 s up to 600 s) allowing measurements of the pedestal and noise for each channel. By sending calibration signals, we are also able to measure the gain and to follow its evolution.
- DUT 2 : Reference ADC on a dedicated board. Here we simply measure the evolution of the output voltage versus the received dose.
- DUT 3 : MARC on a modified MANU board. Using the same acquisition program, data will be taken during and after each irradiation. The two ADCs of the MANU board have been removed and replaced by appropriate resistors; thus the values read by the MARC are restricted to 4095 (32 channels) or 0 (32 channels) only.

DUT 1 & 2 will be irradiated at the same time as shown on figure 5. For DUT 3, the beam size was collimated to a smaller diameter (20 mm) and the modified MANU board was placed in a position where the MARC chip was the only component irradiated.

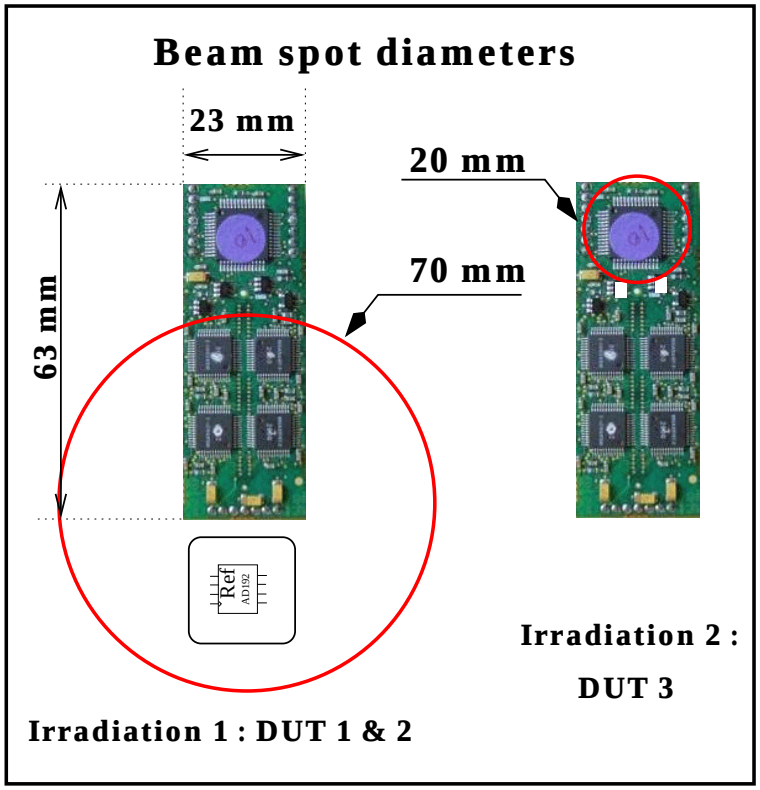

Figure 5: Beam collimation for the two irradiation setups.

The MANU boards need to be powered with 3 voltages, ±2.5 and +3.3 volts; the first ones (±2.5 V) are strongly correlated to the MANAS whereas the second one (+3.3 V) is mainly related to the MARC. For each irradiation, the current consumption on each voltage supply was monitored and limited to prevent SEL.

4.2 Proton beam from CPO

The proton beam delivered by the CPO can be tuned from an energy of 50 up to 200 MeV. Depending on the energy the proton fluence typically varies from 5.0×10^7 cm^{-2}s^{-1} (at 50 MeV) to 1.0×10^8 cm^{-2}s^{-1} (at 200 MeV). Neutron contamination has been estimated at about 1% and beam inhomogeneity to less than 6%. The beam energy was set at 187.5 MeV (initial request was $180 \leq E_p \leq 200$ MeV). The proton flux was higher than expected, reaching during the irradiation a mean value of $\sim 2.0 \times 10^8$ cm^{-2}s^{-1}.

First irradiation (DUT 3), during which a fluence of 3.6×10^{11} cm^{-2} was obtained (21.8 kRad in terms of TID), has been done in 2520 seconds (7 runs of variable duration).

Irradiation of DUT 1 and 2 was done with 1230 seconds of beam time (10 runs of variable duration) achieving a fluence of 2.0×10^{11} cm^{-2} (12.8 kRad in terms of TID).

5 Results

5.1 MANAS

5.1.1 Pedestal and noise evolution

On figure 6 is represented the evolution of the pedestal and the noise versus the proton fluence (and the subsequent dose). The mean value of the pedestal and the noise are averaged over 64 channels (i.e. 4 MANAS), the error bars being the RMS of the distribution. The noise stays

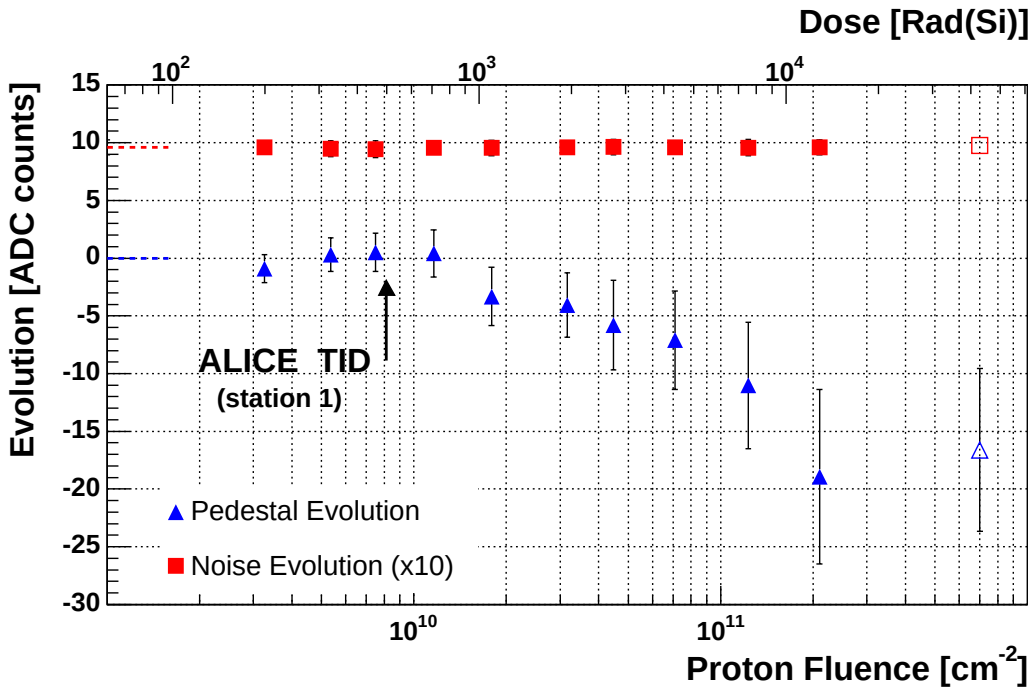

Figure 6: Pedestal and noise evolution of the MANAS versus the dose/fluence (empty symbols correspond to a measurement made 5 days after the irradiation).

remarkably flat during all the irradiation up to a dose of 10 kRad, which can be considered as a very adequate behavior. After a dose of 1 kRad, one can see a decrease of the pedestal values

with respect to their initial values. At the end of the irradiation (TID is close to 15 kRad), the mean value for the pedestal is 19 ADC counts smaller (12 mV), and the values for each individual channels are much more dispersed (note that for a non-irradiated MANAS chip, pedestal values are usually spread over a large range, up to $\sim$ 200 ADC counts).

On this figure is also plotted the result a of measurement made 5 days after the irradiation (empty symbols). We can see that the pedestal seems to recover from the irradiation effects (annealing-like effect).

5.1.2 Gain variation

Gain measurements have also been performed by sending a set of calibration signals into the MANAS and analysing the response of the chips. The calibration signals (0, 150, 300, 450 and 600 mV) were sent in all the channels in parallel through a built-in capacitor of 0.2 pF; this roughly corresponds to an input charge ranging from 0 to 120 fC where sits the most probable value for the maximum charge collected by a single pad of the muon chamber (the value determined from beam tests at CERN is about 60 fC).

Gain evolution is presented on figure 7. It represents the mean values (over 64 channels) of the 3 parameters of the second order polynomial function used to fit the calibration curves.

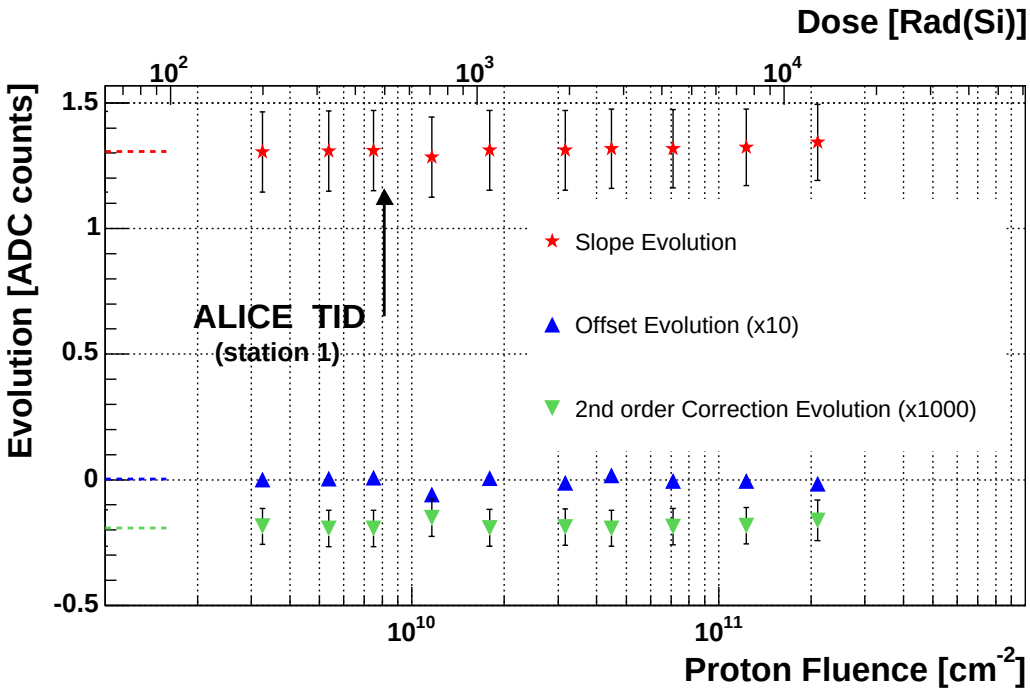

Figure 7: Gain evolution of the MANAS versus the dose/fluence.

The gain of the MANAS chip is linear only in the lower part of its dynamic range, i.e. for an injected charge below 120 fC (whole dynamic range goes up to 500 fC). Above this value, one really needs to add a quadratic term to have a correct parametrization of the gain. Using a first order polynomial function to fit the calibration data taken during our irradiation tests does not change significantly the results; the slope decreases by 10% and the offset parameter

is shifted to a value of ~ 0.3 ADC counts. Most importantly the parameters evolution remains comparable to the one shown on figure 7, i.e. it stays flat with respect to the TID.

5.2 ADC Reference

On figure 8 is shown the output voltage of the component AD Ref192, which provides the voltage reference to the ADC. The output voltage was permanently monitored and periods when the beam was on are indicated on the figure (vertical lines) together with the received dose.

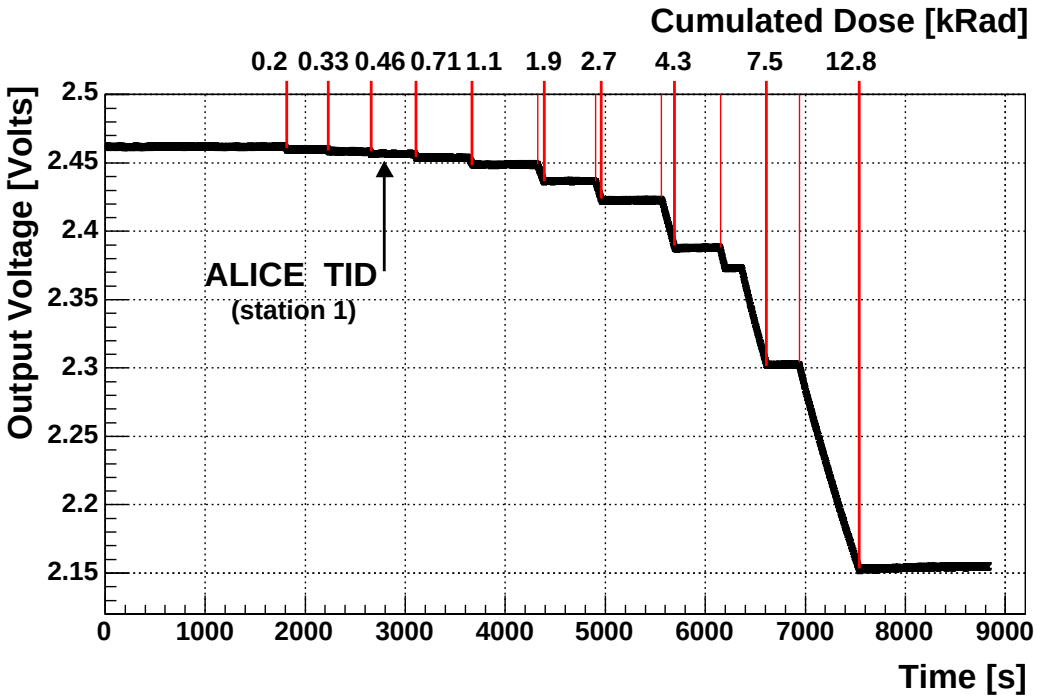

Figure 8: Output voltage of the reference AD192 versus the dose/fluence.

The effect of irradiation is clearly visible: the output voltage drops linearly during every period the beam is switched on. After an irradiation period, the output voltage stays at the lowest value it reached. For a TID of 460 Rad, the voltage drop was only 0.2% (about 5 mV) and 0.3% (8 mV) after 710 Rad. The voltage was measured again 4 days later; we found that its value was back up to the value measured before the irradiation. The component AD Ref192 has been exposed to a TID of 12.8 kRad and had completely recovered from this irradiation after 4 days. During the ALICE experiment, a TID of 500 Rad will be deposed over several years, allowing the component to recover from these small irradiation effects. The voltage reference AD Ref192 is perfectly well suited for our FEE.

5.3 MARC

The most sensitive part of the MARC is certainly the RAM where are stored 64 words of 12 bits; these are threshold values that will be compared to the ADC words for the zero suppression. In order to test this RAM, a file containing 64 words of 12 bits (following a

0xaaa and 0x555 pattern) has been uploaded in the RAM of the MARC chip at the beginning of the irradiation. After each irradiation, this file was downloaded and compared to the initial one; number of bit errors in the RAM has been determined with this procedure and results are shown on figure 9.

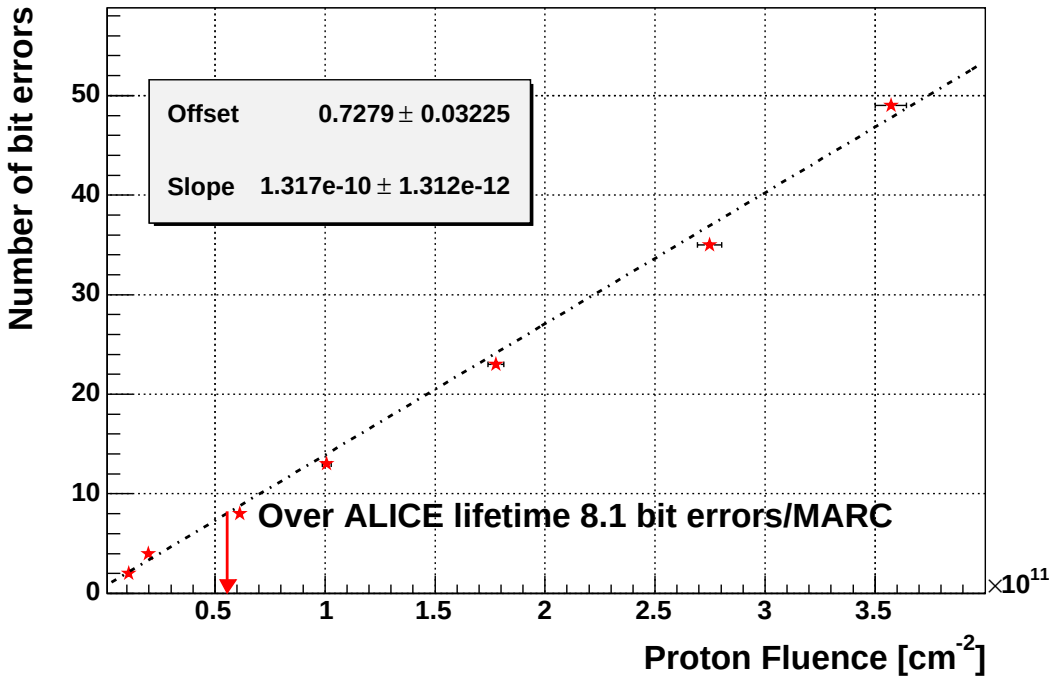

Figure 9: Number of bit errors in the RAM of a MARC versus the proton fluence.

From this measurement, a total of 8.1 errors is expected to occur in the RAM of a MARC under a proton fluence [4] of 5.6×10^{10} cm^{-2}. Considering the total number of MARC in the station 1 (3608), the extrapolation leads to a rate of 23 errors per day; if MARC memories are reloaded every 6 hours (which is the foreseen beam lifetime) this error rate is divided by 4 and it will not have an impact on the data acquisition.

One can push further this extrapolation by considering the entire DFS, i.e. the 5 stations. Tables 1 and 2 give us the total number of MARCs and the hadron fluence for each station; using the SEU cross section from the fit on figure 9, we obtain a total of 56 SEUs per day in the whole dimuon forward spectrometer. With the same assumption on beam lifetime, it means that, after 6 consecutive hours of data taking, a maximum of 16 channels will have a modified threshold value because of SEUs. This number appears to be completely negligible when compared to the 1.1 million of channels of the DFS.

Data were also taken during the irradiation of the MARC. After processing in the MARC, a 12 bits ADC word is addressed and becomes a data word of 32 bits. Due to the modification made on the MANU board the ADC word can only take the values 0 or 4095; knowing the MANAS, MARC and MANU addresses it was easy to check if the data words were corrupted. This has been verified for the all the runs and no dynamics errors were detected.

[4] effects due this proton fluence are equivalent (or more important) to the effects due to the hadron (E_{had} >2 MeV) fluence expected in ALICE as discussed in 3.1. This fluence corresponds to the one received during the 42 months of data taking (10 years of ALICE).

6 Conclusions

The principal result of these tests is certainly the very good behavior we have observed for the components of dimuon forward spectrometer FEE and DAQ.

On the DAQ side, the components already tested by other experiments (CMS,AMS) do not show any significant problems with respect to irradiation that will require to replace them. In order to validate the CROCUS boards (some components still need to be characterized, especially the DSP), irradiation tests will be necessary (probably with neutrons) ans are in preparation.

On the FEE side, the MANAS appears to have a good resistance to radiation: channel noise and gain values stay constant up to a dose of 12.8 kRad. Only the pedestals seem to suffer; after a dose of 1 kRad, values started to decrease and are much more dispersed. For the 4 MANAS tested no SEU/SEL have been observed, leading to an upper limit for the cross section $\sigma_{\mathrm{SEU/SEL}} \leq 0.5 \times 10^{-11}$ cm^2.
MARC results are excellent : the sensitivity to SEU is low ($\sigma_{SEU} \sim 1.4 \times 10^{-10}$ cm^2); the extrapolation leads to a total of 14 SEUs for the entire DFS after 6 hours of continuous data taking (no reset/reload cycle). No SEL have been observed, setting an upper limit for the cross-section of $\sigma_{SEL} < 2.8 \times 10^{-12}$ cm^2.
The reference for the ADC, component AD Ref192, has shown a strong variation of its output voltage with respect to the received dose ($\sim$ 13% decrease after 12.8 kRad) during the iradiation but has completely recovered after only 4 days. ALICE TID is only 500 Rad (or 50 Rad per year), thus the component AD Ref192 is not expected to exhibit any TID effects at such a low dose level.

For both MANAS and MARC, the current cunsomption has stayed constant during all the irradiation and only started to increase after a dose of 12.8 kRad and 21.8 kRad respectively. These doses are extremely high compare to the ones expected in the the DFS : further investigations will be necessary if one would use these ICs at such a high dose.

In conclusion, for the expected levels of radiation (dose and hadron fluence) in the dimuon forward spectrometer, we have seen that the following components: Eprom AMD AM29LV040, FPGA Xilinx Spartan IIE, EPLD Xilinx XC9536XL, ADC AD7476, AD Ref192, MANAS and MARC are perfectly safe to use for FEE and DAQ applications.

We wish to thank the scientists and the director of the Centre de Protonthérapie d'Orsay for making this collaboration possible and fruitful.

Annexe A

From Gy to dE/dx, Irradiation Simulations

- **Units and example**

  The SI unit for radiation is the gray (Gy) which is an energy per unit of mass, 1 joule/kg. The rad is often used and, surprisingly, the conversion is straightforward, 1 Gy = 100 Rad. Rigorously, the dose must be expressed relatively to the absorbing material like 100 Rad(Si) or 100 Rad($Si0_2$). When a particle crosses a material, it deposits energy through ionization: we can speak of LET (Linear Energy Transfer) or dE/dx (energy loss rate). Both are expressed in $MeVcm^2g^{-1}$ or a (sub-)multiple.

  Let's start with the example of the energy loss calculation for a 200 MeV/c proton in 375 μm of silicon. Then, we will determine the TID (Total Integrated Dose) received in 2 hours for a proton flux of 6.0×10^7 $cm^{-2}s^{-1}$.

  $\longrightarrow$ According to Fig.10, one can see that for a 200 MeV proton in silicon, the energy loss -(dE/dx) is 3.86 $MeVg^{-1}cm^2$. Assuming a constant energy loss through all the

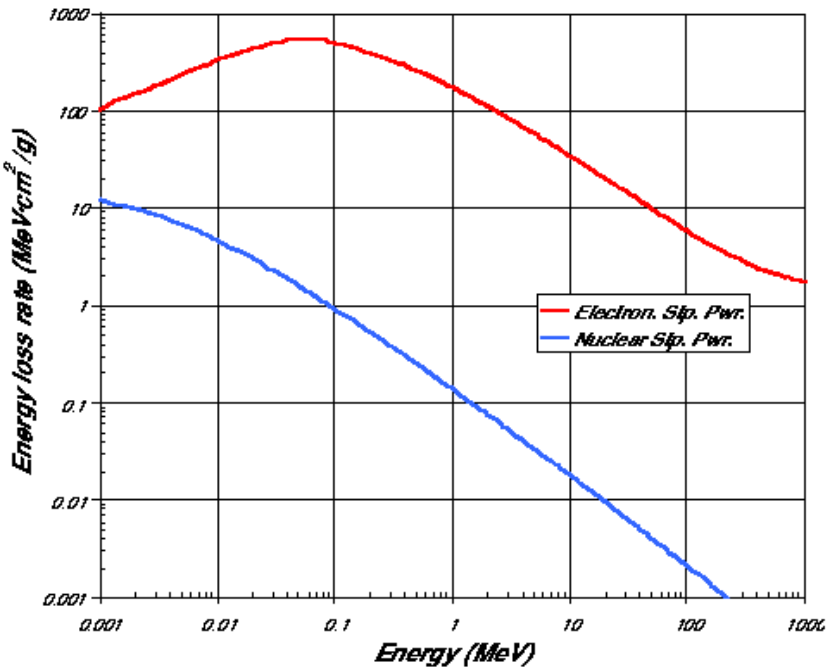

Figure 10: Energy loss of protons in silicon.

0.0375 cm of the material (silicon density is $\rho_{Si} = 2.33$ gcm^{-3}), we obtain:

$$\begin{aligned} -dE &= 3.86 \text{ MeVg}^{-1}\text{cm}^2 \times 2.33 \text{ gcm}^{-3} \times 0.0375 \text{ cm} \\ -dE &= 0.3372675 \text{ MeV} \end{aligned}$$

value that validates our approximation of a constant energy loss since -dE/E$_0$ $\sim 1.7 \times 10^{-3}$.

$\longrightarrow$ 2 hours is 7.2×10^3 s, so we simply write :

$$\begin{aligned} -dE_{\text{tot}} &= -dE \times 6.0 \times 10^7 \text{s}^{-1}\text{cm}^{-2} \times 7.2 \times 10^3 \text{ s} \\ -dE_{\text{tot}} &\sim 14.6 \times 10^{10} \text{ MeVcm}^{-2} \\ &\triangleright \text{ considering the MANAS dimensions } 0.475{\times}0.306{\times}0.0375 \text{ cm}^3 \\ -dE_{\text{tot}} &\sim 2.12 \times 10^{10} \text{ MeV} \end{aligned}$$

The final step is to do the correct conversions, according to :

- 1 Rad $\sim 0.624 \times 10^8$ MeVg^{-1} = C$_1$
- the silicon volume has a mass of $\rho_{Si} \times$ volume = 0.0127 g

numerically :

$$\text{Dose} = \frac{dE_{\text{tot}}}{m_{Si} \times C_1} \sim 27 \text{ kRad(Si)}$$

Going through all these steps is not necessary (but pedagogical) if one use the following equivalent formula :

$$\text{Dose} = \left.\frac{dE}{dx}\right|_{\text{Si}} \frac{\Phi \times t}{C} \text{ Rad(Si)}$$

For 60 MeV protons (energy often used for irradiation tests), the energy loss rate -(dE/dx) is 8.58MeVg^{-1}cm^2; the total dose would be 60 kRad in that case.

- **Simulations**

Step by step or *angstrom by angstrom*, it is possible to compute the energy loss of particle through different layers of materials. To do so, one can use a really convenient program SRIM (Stopping Range of Ions in Matter) [SRIM]. Usually, irradiation tests are performed on an IC in its package, i.e. a *plastic* container. The energy loss through the lead frame is usually the most important and should be described precisely in simulations.

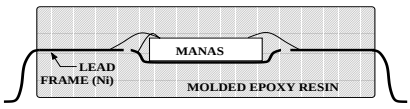

A scheme of the 48 pins TQFP package is drawn on the left: the MANAS IC, in the middle, is bonded to connexions pads extending outside the package. The surrounding material can be described in simulations by a simple epoxy.

Once this geometry is implemented in SRIM, we can simulate a flux of protons and determine the energy loss in the different layers; results are represented on Fig. 11 for two energies.

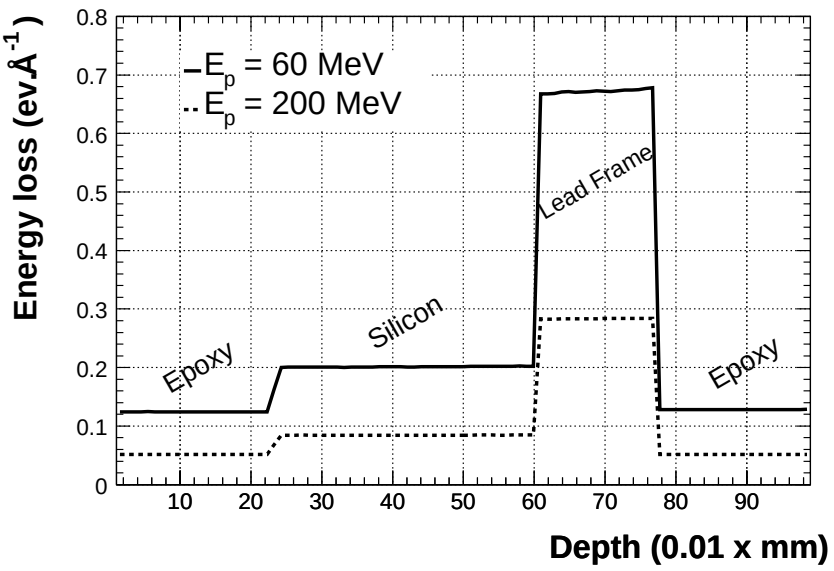

Figure 11: Energy loss of 60 and 200 MeV protons in a *toy* IC model.

Here the energy loss rate is expressed in $\mathrm{eV\AA^{-1}}$ which, in more convenient unit, is equivalent to 100 $\mathrm{MeV cm^{-1}}$. SRIM simulation gives an energy loss for the proton of 0.2 $\mathrm{eV\AA^{-1}}$ equivalent to 20 $\mathrm{MeV cm^{-1}}$; one can divide this value by the silicon density and obtain an energy loss of 8.6 $\mathrm{MeV g^{-1} cm^2}$ (in agreement with the curve of figure 10).

As an example, the same simulation has been run with 200 MeV Argon ions (see Fig. 12); the energy loss in silicon is almost 300 times higher than the one of 200 MeV protons. Heavy ions beam are particularly well suited to trigger Single Event Effect (as explained in Annexe B) and are an important tool to test radiation hardness of space devices.

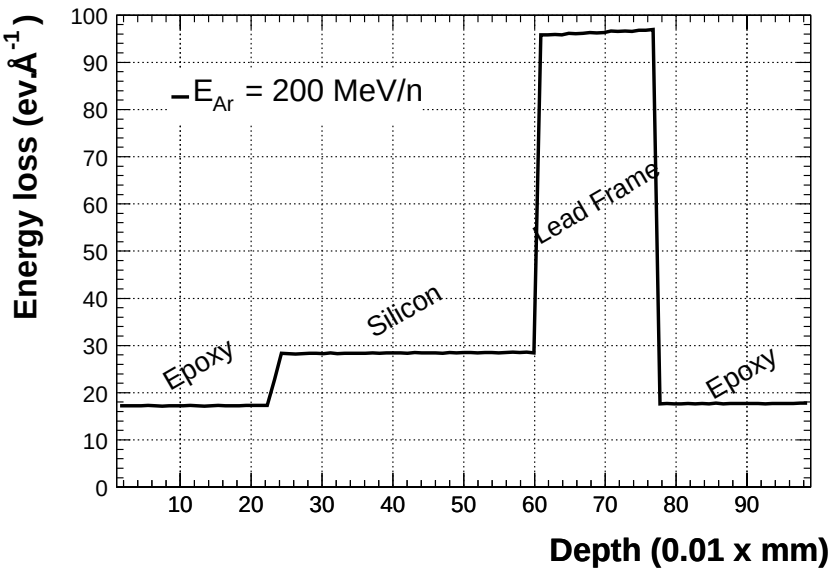

Figure 12: Energy loss of 200 MeV Argon ions in a *toy* IC model.

Annexe B

Reminder on radiation damages

Radiation damages have been extensively studied and numerous detailed publications are now available. Thus the following list (extracted from a very complete and accessible report [Fac03] and a more technical one [Den00]) will stay at a basic description level, aiming to help the reader to separate the different types of damages and how to study them.

- **Cumulative Effects :** gradual effects taking place during the whole lifetime of the electronics exposed in a radiation environment.
  - TID (Total Integrated Dose) is a generic term to regroup the effects related to ionization. The dose is deposited by the particles passing through the materials constituting the electronic device. At LHC these particles are charged hadrons, electrons, gammas and neutrons (the last two are not directly ionizing but they can induce ionizing energy deposition).
    The heart of TID is the energy deposition in the silicon dioxide, because the electron-hole pair created in this material do not recombine in a very short time. In the presence of an electric field in the oxide, a great amount of pairs does not recombine and both electrons and holes start to drift in the electric field (we can notice here the importance of having bias on tested components since ionization would not have the same effects without the electrical field). Electrons, with a much

higher mobility, can easily leave the oxide. Holes instead can be trapped in defects centers in the oxide. Additionally, this process can create (or activate) defects at the silicon-oxide interface.

The charge build-up and the activation of the defects are the two reasons for device degradation induced by TID.

– Displacement damages arise from particles producing Non Ionizing Energy Loss (NIEL). The involved mechanism is related to collisions (elastic diffusion, electromagnetic interaction) in cascade on the atoms of the semiconductor lattice, produced by either a *massive* incident particle (n, p or ion) or secondary particle issued from elastic diffusions or nuclear reactions. Along the tracks of these particle and also at the end of these tracks (the so-called terminal cluster where a particle stop and loses all its energy through multiples collisions/interactions), defects in the lattice are produced (vacancies, interstitial, etc...). The major effects are a decrease of the minority and mobility carrier lifetime, an increase of the resistivity (because the concentration of majority carriers decrease). Type inversion might also occur in high resistivity material which is only used for detectors.

  Bipolar devices can be affected by displacement damages whereas MOS (transistors or capacitors) devices are not. Displacement damages effects are generally negligible below a proton fluence of 3×10^{10} cm^{-2} for PNP transistors (for 50 MeV protons). Above 3×10^{11} cm^{-2}, the displacement effects start to be noticeable also for the NPN transistors. Moreover, data available in the literature indicate that 50 MeV protons are about 1.75 times more damaging than neutrons (1 MeV equivalent).

  To observe specifically the effects of displacements, one should performs two irradiation tests; one with a gamma source (which does not generate displacement damages) and the other with a proton beam. It is not unusual to see differences on a particular observable (output of a voltages regulator for instance); a *normal* (wrt to the TID) evolution is seen during the gamma irradiation but during proton irradiation, large deviation might happen at a given fluence. This phenomenon is called a catastrophic failure because of its unpredictable occurrence when only γ-irradiation tests have been made.

- **Single Events Effects :** very localized event induced by a single particle (whilst TID and displacement damages are gradual cumulative effects). The mechanism can be explained as follow: a single ionizing particle crossing a device will generate a large number of e^+e^- pairs along its track. If the track passes in a space charge region (a reversed bias junction for instance), the junction field lines will propagate along a portion of the track (*funneling effect*) and charges will then quickly drift onto the junction. The junction can either be a cell like a capacitor (charges trigger an upset in DRAM and error in analog memory) or a MOS transistor (the subsequent transient pulse triggers an upset in SRAM and error in logic circuit).

  Not all the particles deposing energy in the semiconductor will induce SEU. Only the energy deposited in a range sufficiently close to the sensitive node can be collected and eventually lead to an upset. Therefore, we define a Sensitive Volume, which correspond roughly to the volume where the charges can be collected and actively participate to SEU. For an IC, the depleted (implanted) region has a very small thickness (on the order of 1 or 2 μm) but charges can still be collected over a much larger depth (the *funnel region* which can extend up to 100 μm).

Heavy ions will can create enough charge in silicon to trigger a SEU. At LHC, the biggest source of SEU will come from nuclear interaction of an high energy particle (p or n) with a nucleus then the secondary ion issued from the reaction has a certain probability to create SEUs. For instance, neutron above 4 MeV can induce reactions in Si and thus start at a really low energy to trigger SEUs.

- Transient and static errors are frequent in analog circuits, or in combinatorial logic. The generated signal are asynchronous, they can propagate through the circuit during one clock cycle and also sometime propagate a latch and become static. Static errors overwrite information stored in the circuit; they can be corrected by outside control by power cycling the IC or rewriting the information.
- Permanent errors (destructive) can cause the failure of the whole circuit. They cannot be recovered unless detected at their very beginning in some cases; for Latchup for instance, powering off fast enough the IC might interrupt the destructive mechanism and bring back the circuit to functionality. Lachtup are likely to occur in CMOS and bipolar ICs.

  Another destructive effect is the Single Event Gate Rupture which can happen in MOS device **when they are off**. A ionizing particle passes through the gate oxide and generates a bias across the oxide; a high instantaneous current is generated and breakdown of the oxide might happen. The resulting (permanent) damage is a short between the gate and the channel.

  Finally, we will just mention the Single Event Burnout that can occur in power MOS or BJT.

- **Cross Sections**

  If we consider a proton beam, then the device cross section for SEU is simply :

$$\sigma = \frac{N_{events}}{\Phi} \quad (\mathrm{cm}^2)$$

  where Φ is the fluence (in case of heavy ions beams, one should use $\Phi \cos\theta$ where θ is the incidence angle).

  In the reference [Huh00], Huhtinen and Faccio propose a computational method to determine the SEU rate in an accelerator environment. In this work, they show that an irradiation with protons directly gives an estimate of the SEU rate at LHC: the measured cross-section at an energy of about 60 MeV or more, multiplied by the total hadron flux (above 20 MeV) foreseen in the position of interest in the detector, gives the expected upset rate.

- **From Space to LHC environment**

  Many electronic devices are tested for the space environment; in this case, heavy ions are the predominant source of ionizing particle. Losing a significant amount of energy when crossing the device, they create enough charges to trigger a SEU.

  The mechanism is different at LHC where ionizing particles are high energy hadrons (mainly pions, protons neutrons), hence unable to deposit enough charges to create an SEU. Nevertheless, through nuclear interactions (elastic but also mostly inelastic) they can communicate enough momentum to another nucleus in such a way that this recoil nucleus (or any reaction product) will be able to induce a SEU. Thus, extrapolation of irradiation results from heavy ions beam to high energy hadrons will require :

- all the p-Si $\longrightarrow$ X cross sections,
- the full cascade reactions from the initial p-Si interaction
- the energy loss of all the products of the reaction in the IC volume

Up to now, there's is no clear method to do the previous calculation. Some results about SEU cross-sections, for devices used in the dimuon forward spectrometer electronic, are available from heavy ions beam tests but unfortunately they can not be translated into the LHC environment.

References

[ALI] Technical Design Report & Physics Performances,
http://alice.web.cern.ch/Alice/AliceNew/collaboration/documents/TDR.htm
http://alice.web.cern.ch/Alice/AliceNew/website/files/presentation/2004/QM2004/YSQM2.ppt

[Bun03] K. Bunkowski et al.,
Radiation tests of RPC trigger electronic components
http://hep.fuw.edu.pl/cms/esr/docs/RadiationTests.pdf (2003).

[CPO] http://www.protontherapie-orsay.fr/

[Den00] M. Dentan,
Radiation effects on electronic components and circuit
http://atlas.web.cern.ch/Atlas/GROUPS/FRONTEND/WWW/RAD/RadWebPage/
Tutorial/Coursedentan1.pdf
Coursedentan2.pdf is also available at the same address.

[Fac03] F. Faccio,
Radiation effects in the electronics for CMS
http://lhcb-elec.web.cern.ch/lhcb-elec/papers/radiation_tutorial.pdf

[Huh00] M. Huhtinen and F Faccio,
Computational methods to estimate Single Event Upset rates in a accelerator environment
Nucl.Instrum.Meth.A450:155-172,2000.

[Lin00] B. Bylsma, L.S. Durkin, J. Gu, T.Y. Ling and M. Tripathi
Results of Radiation Test of the Cathode Front-end Boards for CMS Endcap Muon Chambers
http://lebwshop.home.cern.ch/lebwshop/LEB00_Book/rad/ling.pdf (2000).

[Mor02] A. Morsch and B. Pastircak,
Radiation in ALICE Detectors and Electronics Racks
ALICE Internal Note, ALICE-INT-2002-028 1.0.
Updated simulations presented at ALICE Technical Board, Feb. 23rd 2004.

[Mor04] A. Morsch, Private Communication.

[NA50] NA50 Collaboration,
Evidence for deconfinement of quarks and gluons from the J/psi suppression pattern measured in Pb-Pb collisions at the CERN-SPS
Physics Letters B 477 (2000) 28.

[QM04] http://www.lbl.gov/nsd/qm04/program.html

[RHIC] http://www.bnl.gov/RHIC/

[SRIM] http://www.srim.org

[Tim01] R. Timmer
Radiation tests on electronics components for the AMS detector
Private Report (2001).